International Journal of Engineering Trends and Technology
ISSN: 2231 – 5381 / https://doi.org/10.14445/22315381/IJETT-V70I4P207
Volume 70 Issue 4, 82-94, April 2022

Original Article

Feasibility of VOF-FEM Coupling to Study the Wave Impact on a Sloping Seawall

Dabir V. V[1], Shinde S. R[2], Khare K. C[3], Londhe S. N[4]

[1,3]*Department of Civil Engineering, Symbiosis Institute of Technology, Symbiosis International (Deemed University), Pune, Maharashtra, India.*
[2]*Symbiosis Institute of Technology, Symbiosis International (Deemed University), Pune, Maharashtra, India.*
[4]*Department of Civil Engineering, Vishwakarma Institute of Information Technology, Pune, Maharashtra, India.*

[1]vaishnavi.dabir@sitpune.edu.in

Received: 13 February 2022 Revised: 28 March 2022 Accepted: 30 March 2022 Published: 26 April 2022

Abstract *- Seawalls are structures constructed along the coastline for effective energy dissipation. It is imperative to study the wave forces on the structure and response thereof for designing such structures. The research on the performance of coastal structures connotes the utilisation of the Irribaren number (ξ), which is a function of wave parameters and the slope of the structure over which the wave attacks. It is an uphill task to investigate the effect of changing the slope of seawall over the wave parameters experimentally. Therefore, the use of a numerical tool can provide an agile alternative. To choose the appropriate method for this analysis, a thorough literature review is performed. From the inferences, the VOF-FEM coupled tool is selected to address wave structure interaction studies for coastal structures wherein no transmission of wave and thus no mixing of the incident and reflected flow in the computational domain is expected. The Numerical model is further tested to study the effect of the inclination of the structure over the run-up pressure experienced by the structure. The results matched well with an experimental trial performed and with previous work in similar conditions from the literature. The results are presented, and the feasibility of using VOF-FEM coupling for shoreline non-wave transmitting structures is discussed.*

Keywords *- Coastal, Seawall, FEM-VOF coupling, Wave force, Wave Structure Interaction.*

1. Introduction

Coastal erosion due to the impact of waves is prominent on unsupported coasts. To protect the coastline from erosion, the dissipation of wave energy is essential. This can be achieved by the construction of seawalls, breakwaters, groins, etc., which are constructed along a coastline. For designing such structures, it is imperative to study the wave forces on the structure and note the response thereof. Such wave structure interaction studies are carried out using analytical, experimental, and numerical techniques [1]. The research to date focuses on two primary elements in the performance of the structure, the first being the energy dissipation, which can be denoted by wave dissipation, transmission, or pressure experienced by the seawall over its surface length; the other being the surf similarity parameter (Irribaren number). The Irribaren number is a function of the slope of the structure and the incident wave parameters.

The majority of the research to date focuses on varying the wave parameters in the Irribaren number term [2]. This, of course, helps to comment on the performance of the given structure over different wave conditions. However, to understand the role of structure in energy dissipation, the parameters of the structure need to be identified and varied, perhaps to determine the most prominent element. In this study, a smooth non-porus slope of the structure is taken into consideration. Few researchers have conducted experimental investigations on the seawall with varying slopes to assess wave reflection performance. [3]–[6] However, no numerical study is found to be focusing on the utilisation of a numerical tool for assessing the effect of changing slopes of seawall over energy dissipation. Once it is achieved, it would be possible to widen the possibilities of research in this domain.

Among the analytical procedures, the commonly adopted methods are the use of Morison's equations, Navier-stokes equation, Lagrangian method, etc., to predict wave conditions, and the Van der meer equation is used for structural design. For complicated cases, it would be tedious to solve the equations analytically considering the time constraints. Experimental investigations, on the other hand, are scaled-down studies that give a visual representation of the performance of the structure. In such investigations, certain properties like the dimension of sand particles or the size of the opening in the geotextile of the prototype cannot be scaled down as per the dimensional analysis. It is evident that there would be some misappropriation and, therefore, errors in the solution. Therefore, numerical modelling tools appear to be a viable option that works on the basis of fundamental analytical equations and provides a visual representation of the problem under consideration. The prime benefit of incorporating a numerical model is the

possibility of the selection of scale. Full-scale simulation is possible once the model is established with successful training. The model can be validated using experimental results, which are usually designed at a smaller scale or by analytical established equations. The scale of the numerical model is dependent on the software and hardware configurations of the user device since it directly affects the computation time. In this paper, a thorough literature review is carried out for shortlisting an efficient computational system for wave structure interaction studies for seawall structure. Thereafter a bibliometric expanse of the VOF-FEM method is conducted, followed by an experimental and numerical trial on a non-overtopping structure using this technic.

1.1 Literature Review

Various numerical tools exist for modelling wave parameters. For structural modelling parameters, it can be accomplished via finite element modelling, wherein the response of the earth structures, geosynthetic sand containers, etc., to loading conditions can be checked. However, for checking the structural response to the impact of waves – the characteristics of which are in turn affected by the configuration of the structure over which the waves interact, the coupling of two systems in a numerical tool will be ideal. A background literature survey is essential before the selection of an ideal tool for the study.

From the expanse of literature, the most commonly incorporated numerical methods for computation in this domain are determined to be Nonlinear Shallow Water Equation (NSWE), Smoothed particle hydrodynamics (SPH), Navier–Stokes equations (or RANS equations), Computational fluid dynamics (CFD), The Reynolds-averaged Volume of Fluid (VOF), Finite element methods (FEM) etc. The Nonlinear Shallow Water Equation (NSWE) area set of hyperbolic partial differential equations that define the flow below a pressure surface in a fluid (sometimes, but not necessarily, a free surface). Nonlinear shallow-water equation is used for simulating non-hydrostatic, free-surface, rotational flows in one and two horizontal dimensions [7],[8], [9], [10], [11], [12]. Simulation of dynamics of continuum media, such as solid mechanics and fluid flows, is carried out using Smoothed-Particle Hydrodynamics (SPH) [13], [14], [15]. It is based on the mesh-free Lagrangian method. SPH provides an underestimated solution for resolving small-scale motions and predicts a power spectrum that is far too steep [12], [16]. The basic objective of computational Fluid Dynamics (CFD) is to solve approximately the flow and basic equations that provide the movement and other characteristics of the flow, but it is difficult for Multiphysics (Computational Fluid Dynamics) CFD to solve large simulations [17], [18], [19],[20], [12].

The Reynolds-averaged Navier–Stokes equations (or RANS equations) are related to time-averaged equations of motion for fluid flow. Generally, turbulent flows are described using RANS [21], [22], [23]. k-eps and k-omega are not competent for the effect of rotation on turbulence, and therefore they give bad results when there is swirl or streamline curvature [24], [25], [26]. Primarily, the Finite Element Method (FEM) or Finite Element Analysis (FEA) is used for solving engineering problems. For obtaining a solution for the domain, it divides a larger problem into smaller, naive parts that are called finite elements[27],[28],[29]. The volume of fluid (VOF) method is a free-surface modelling technique, i.e. a numerical technique for tracking and locating the free surface (or fluid-fluid interface).

Multiphase flow settings are modelled using the Volume of Fluid (VOF) model is required for the generation of waves. VOF model is a surface tracking method that works very well for multiphase flows where a distinct interface is present. The free surface between water and air is provided with finer mesh for obtaining high accuracy of solution[30],[31],[32]. Implicit function asserts continuity equation with the momentum equation, solving for the volume fraction and flow field at the same time. For a particular phase, the main assumption in VOF approach is that the volume fraction is always between 0 and 1. That is, there can be no empty regions, and each control volume must be assigned with one or more present phases.

Many researchers have studied the wave structure interaction for offshore structures with the VOF-FEM coupling [12],[19],[25]. Few researchers have studied shoreline structures, but the study focused on analytical and experimental results. [33]–[35]. The studies focus on the effect of waves on structure with variation in wave heights, water depths, and wave periods. However, less attention is given to the effect of structural parameters, namely slope of the structure, friction with the surface, the permeability of the structures, the thickness of layers, etc., on the overall hydraulic performance of the seawall. No research to date covers the aspect of structural variation of the shoreline structure. This may be due to the complexity and physical efforts required for experimental investigation. Hence, Numerical tools may come in handy for addressing the effect of these parameters for noting the overall hydraulic response of the structure.

[9] compared the numerical results of SWASH with various cases of laboratory data and inferred that a good amount of computational time is saved in SWASH. [36] investigated ocean waves using the commercial software tool 'FLUENT', which is based on the Navier-Stokes equations. It is applied to viscous, incompressible fluid along with the Volume of Fluid (VOF) method. As compared to the physical model experiments, this numerical model is more pliable since the dimensions of the wave tank can be altered as per the demand of the situation. [17] simulated both linear waves and linear deepwater waves using the commercially available yet commonly used finite volume package ANSYS CFX (Release 12.1). From the results, the author concluded that the deepwater wave generated by CFD is in very good agreement with Linear Wave Theory. Certain criteria are required for the selection of a particular wave theory, but they are not generally

specified because no simple theory predicts all wave properties satisfactorily. In general, the simple Airys linear theory is suitable if the wave has a small steepness, the sea is multi-directional, the wave spectrum is broadly banded, or the structural dimensions are such that the inertial forces are dominant than the drag forces. Experiments in the laboratory and those in the sea have shown the adequacy of the linear theory in general, and in deep water that of, the Stokes fifth-order theory is used to predict particle kinematics. Dean's higher-order analysis gives better results for the steeper waves. Considering the convergence of the series terms, the Stokes theory is useful when water is deeper than 10% of the wavelength, while the Solitary theory is ideal if the depth of water is shallower than 20% of the wavelength. In between, the Cnoidal theory would give converging results. Experimentally based guidelines are given in [37]. The selection of appropriate wave theory among the Linear, Cnoidal, Stokes, and Dean's theories is initiated starting from the given values of wave height (H), period (T) and water depth. Next, the non-dimensional quantities are determined, viz., $d/(gT^2)$ and (H/gT^2). From the former quantity, continue on absicca until the point of intersection with the vertical line is obtained. This should correspond to the known $d/(gT^2)$ value. The location of this junction point signifies the correct theory to be chosen.

[16] compared the numerical results of DualSPHysics is a numerical tool based on the Smoothed Particle Hydrodynamics. It permits feigning real-engineering difficulties that include composite geometries with a great resolution in a reasonable computational time. DualSPhysics with experimental data. Results show satisfactory agreements between numerical results and experimental data. [21] used an open-source code – 'OPEN-FOAM', which solves RANS (Reynolds Averaged Navier-Stokes) to simulate the wave interaction with a series of piled structures. A comprehensive pressure and velocity profiles are obtained for each time step, therefore indicating further requisite of validation of the code. [12] compared three different numerical models DualSphysics, SWASH, and Flow-3D, for the study of wave overtopping [38] as well as the impact on a seawall. The results of overtopping obtained from SWASH are 10 times the lesser value even after keeping the same incident wave height. It is also noticed that experimental and numerical overtopping results of flow 3D are synchronised reasonably well. Both DualSPHysics and FLOW-3D display reasonable estimates of the wave impact on the sea wall. [39] compared two numerical models, Fluent and Flow-3D, which are based on the Navier-stokes and VOF equations. The equations are used to generate regular waves in a numerical wave tank. Similar results are obtained; however, the results from fluent had a slight difference from theoretical results but are more accurate in wave crest capturing. [40] used CFD to simulate a new wave boundary condition for extreme waves and wave-structure interactions. The validation includes comparing theoretical and experimental observations. Overall, the results approved the OPEN FOAM model as well placed, which can be used as an extension to many coastal engineering applications and to simulate a wide range of nonlinear wave conditions. [41] used ANSYS fluent 16.0 for the development of a numerical wave tank (NWT). Precise fluid velocity profiles and defining free surface elevation ensure the use of NWT for future studies to assess the performance of wave energy converters, thus resulting in device design optimisation. The mesh size is varied, and the results were compared for free surface elevation and horizontal and vertical fluid velocities. [11] examined the applicability of the lucidified depth-integrated wave transformation model SWASH for estimating wave overtopping over impervious coastal structures, especially in shallow foreshore regions. SWASH being a depth-integrated model, any arrangement in the vertical direction using solids cannot be applied. [26] focused on the assessment of the performance of 'OPEN-FOAM' when applied to nonlinear wave interactions using varying wave conditions onto offshore structures. The numerical results for wave interactions are compared with physical experiments. The developed numerical model worked well for all the test cases discussed in this paper. Repetitive stimulation can be done using NSWE, which gives good results for wave transformation and overtopping, but it takes a longer time to run the calculation. The main advantage of the SPH technique is that it can solve complex problems. CFD differs from other fluid dynamics software because it can give results for flowing fluid surfaces that are modelled with the VOF technique. The main con of this technique is that computing large simulations requires higher version computers, and getting access to them could be difficult. RANS require a lesser number of preliminary speculations. The disadvantage of the RANS model is the substantial computational cost. Most sophisticated models for multiphase flows, such as complicated viscous flow and turbulent flow, can be solved by using FEM is one of the leading advantages. NSW overestimates the overtopping results by almost 10 times more than the other software. While the SPH model has averaged deviation of overtopping rate is about 6.8% which is also slightly more. CFD results are not well synchronised, and RAN's model has a stiffness limit up to 0.033, whereas this limit in FEM is 0.1420. Only the FEM technique can use for all types of numerical problems with well-synchronised results of overtopping and complex time and spatial evaluation of flux.

Hence, it is inferred to use Ansys, which has a provision to couple the systems of the VOF and FEM domain in the same platform. While in other software, it is not possible to use both VOF and FEM approaches at a time. [42] Conducted a thorough literature review to select the appropriate tool based on the accuracy of the results along with the pros and cons of each of the numerical tool alternatives. It is indicated that Ansys could be a suitable alternative considering the ease of availability and the possibility of effective simulation of the structural parameters. Ansys is one of the most used tools in an academic environment and possesses many of the aforementioned advantages.

The literature indicates a promising scope of research in VOF-FEM coupled computational systems for wave structure interaction studies on seawall structures. This paper further aims to incorporate VOF-FEM coupling for seawall for analysing wave-structure interaction. Ansys is selected after a thorough literature review after ascertaining the possibility of simulation of coupled VOF-FEM system. Although the Volume of the Fluid approach has been used for coastal structures like breakwaters, the uniqueness of this study is to completely reflect the waves without overtopping and allow for no transmission. Also, no literature has been found focusing on the utilisation of the tool in the coastal shallow water environment structure. Ample literature focuses on an analytical and experimental investigation of shoreline structures. However, a scanty amount of work is carried out on shoreline non-overtopping structures. Thus, setting up the numerical environment in Ansys and validating the results via an analytical and one-step experimental approach is presented in this paper.

2. Methodology

A numerical tool requires calibration using known boundary conditions and parameters [43]. For achieving this, an experiment is performed in a 10-meter long wave flume (Fig. 1). Similar scale experimental studies can be seen in [44],[45],[46].

Fig. 1 Wave Flume used in experimentation

Thereafter, the numerical tool is set up and validated using analytical established empirical equations. (Fig. 2), The experimental program comprised of measuring run-up

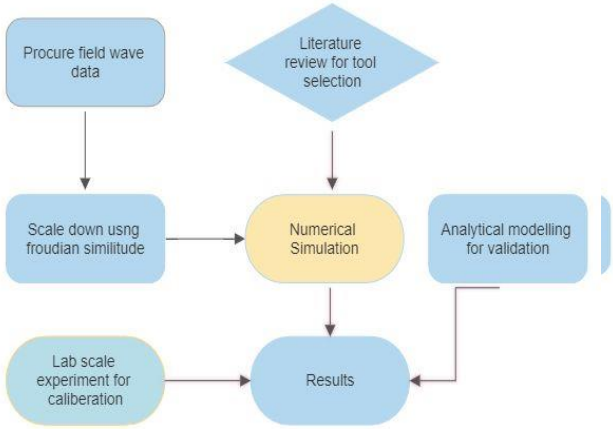

Fig. 2 Methodology of the research

on the seawall with a smooth, impermeable slope. The wave-maker is a mechanical flap-type generator, capable of generating regular waves of height (H) ranging from 0.07-0.15 m, at mean water depth (d) = 0.4 m, wave period (T) = 1- 2sec. The wavemaker is devised using the procedure described in [45]**.** The wave height generated at a given water depth for this setup is observed by undertaking empty flume runs and measuring the incident wave height using a ruler attached at three locations one meter apart in the flume.

A 0.5 HP motor is attached to the wavemaker flap (Fig. 3) to have control over the generation of regular waves. The formula utilised for wavemaker movement and motor capacity [28] is as follows:

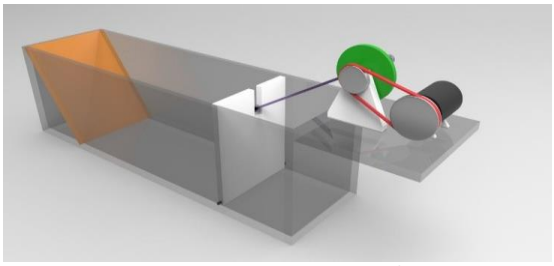

Fig. 3 Wavemaker setup in the flume

Relative Depth

$$kh = \frac{2\pi h}{l} \quad \text{.....(1)}$$

Wave Height to stroke ratio

$$\frac{H}{S_\circ} = \frac{4Sinh^2 kh}{Sinh\ 2kh+2kh} \quad \text{.....(2)}$$

The mean power to generate this wave

$$\frac{P_0}{\left(\frac{\rho g h {S_\circ}^2}{T}\right)} = \frac{\pi}{kh}\left(\frac{\tanh kh}{\sinh 2kh+2kh}\right)\left[\sinh kh + \frac{1}{kh}(1 - \cosh kh)\right] \quad \text{.....(3)}$$

Where, Kh = Relative depth, H= Wave height, h = water depth, T= Time period, L= Linear theory wavelength, H/So= Wave height to stroke ratio, and Po= Mean power to generate the wave.

The amplitude and frequency at which the wave height is generated are recorded and set during the actual experimental trials. Since the study had to be conducted using regular waves, this method deems sufficient for control over incident wave generation. A sample seawall dimension of 10 m length, 1m height, and unit width is considered and reduced to scale using a froudian similitude.

A model is in similitude if it has three basic requirements of geometric, kinetic, and dynamic equality. If these three equalities match those of the system being modelled, then the model has similitude. The concept is mostly used in hydraulic and aerospace engineering. Kinematic similarity shows a comparison of particle motion in the model and prototype. The dynamic similarity between two kinematically and geometrically similar systems necessitates the complete vectorial forces ratios in the two systems to be the same. The scale is decided from the ratio of prototype dimension to the dimension of the model from different iterations as follows,

Iteration No. 1
H = 2.1 m, d = 10 m and T = 10 sec
For 1:10 scale

$H_m = \frac{H_p}{Scale} = \frac{2.1 \times 100}{10}$ =21 cm

$d_m = \frac{d_p}{Scale} = \frac{10 \times 100}{10}$ = 100 cm

$T_m = \frac{T_p}{\sqrt{Scale}} = \frac{10}{\sqrt{10}}$ = 3.16 sec

Iteration No. 2

H = 2.1 m, d = 10 m and T = 10 sec

For 1:20 scale

$H_m = \frac{H_p}{Scale} = \frac{2.1 \times 100}{20}$ =10.5 cm

$d_m = \frac{d_p}{Scale} = \frac{10 \times 100}{20}$ = 50 cm

$T_m = \frac{T_p}{\sqrt{Scale}} = \frac{10}{\sqrt{20}}$ = 2.24 sec

Iteration No. 3

H = 2.1 m, d = 10 m and T = 10 sec

For 1:30 scale

$H_m = \frac{H_p}{Scale} = \frac{2.1 \times 100}{30}$ =7 cm

$d_m = \frac{d_p}{Scale} = \frac{10 \times 100}{30}$ = 33.33 cm

$T_m = \frac{T_p}{\sqrt{Scale}} = \frac{10}{\sqrt{30}}$ = 1.82 sec

Therefore in iteration 3, the range of values is possible to be generated in the existing wave flume. Hence, a scale of 1:30 is adopted for the experimentation program since it is the best possible scale which matches with Froudian similitude in the wave flume [47]. Table 1 shows the geometrical field and lab dimensions to satisfy the similitude [4].

Readings of the wave pressure are measured at the surface of the seawall using a pressure transducer of range 0-300 millibar range. The transducer assembly consists of a stainless-steel diaphragm attached to the pressure sensor using a flexible tube filled with a viscous fluid. The diaphragm resonates due to the pulsating waves, and the pressure due to oil in the tube is sensed by the transducer, which transmits the pressure in terms of voltage displayed digitally. The pressure is converted using a conversion graph of the device, as shown in Fig. 4.

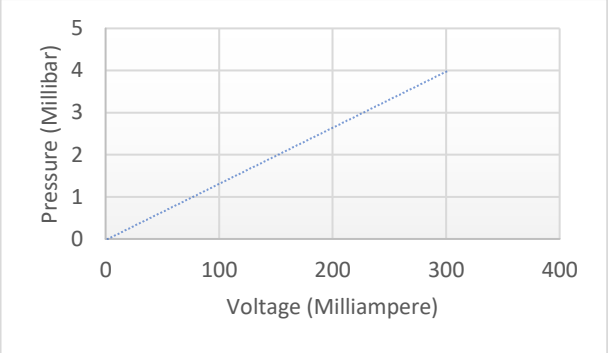

Fig. 4 Conversion curve for pressure transducer

Table 1. Field and corresponding lab geometrical dimensions

Wave Parameters	Lab-scale model	Field Dimensions
Wave Height	7 cm	2.1 m
Water Depth	33.33 cm	10 m
Wave Period	1.82 sec	10 sec
Type of Wave	Non-breaking	Non-breaking
Crest Height	40.62 cm	12.184 m
Crest Width	10.67 cm	3.20 m
Toe Width	13.33 cm	4 m
Toe Depth	14 cm	4.2 m

2 sensors were placed on the upper 1/3rd surface area of the seawall after gauging the location of wave impact via empty trial on the seawall. Readings of pressure values corresponding to 100 regular waves were noted and averaged out for obtaining the wave pressure value. These readings are utilised for input and calibration of the numerical model.

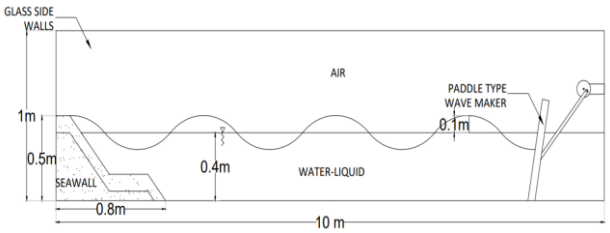

Fig. 5 Schematic sketch of the experimental arrangement

2.1 Numerical Investigation

The surf similarity parameter is calculated numerically using the Iribarren number (equation 4) for varying slopes of the seawall. The shore protection manual prescribes a range of 1:1.5 to 1:3; however, the 1:3 slope would be economically expensive and hence is not considered. The slope selected lies in the range of 1:1 to 1:2.5. In the selected range, the angles for investigation selected are 40º, 45 º,50

^{o},55 ^{o}, and 60 ^{o}. Table 2 shows the length of the seawall for different slope angles keeping the height at 0.5 m. The width of the flume is 0.5 m. Hence it was decided to keep the height equal to the width for ease of setup construction.

$$\xi = \frac{\tan \alpha}{\sqrt{\frac{H}{L_0}}} \quad \text{..... (4)}$$

Where,
ξ= Surf similarity parameter or Iribarren parameter or Iribarren number, α = Slope of Seawall (degrees), H = Wave Height (m), L_0 = Wavelength (m).
The wave data is obtained from INCOIS (Indian National Centre for Ocean Information Services). Readings of the western Coast of India obtained from the Ratnagiri wave buoy have been considered as a sample in this study. The significant wave height is 2.1 meters which is incorporated for the study as a regular wave.

Table 2. Dimensions of seawall for different slope angles in the numerical simulation

Sr. no.	Slope	Height (m)	Length(m)
1.	40^0	0.5	0.85
2.	45^0	0.5	0.848
3.	50^0	0.5	0.800
4.	55^0	0.5	0.77
5.	60^0	0.5	0.76

For the numerical investigation, the VOF approach is used for the generation of waves and is coupled with FEM for obtaining the response of the structure.

In the structural domain, the 3D geometry of the seawall is set up as per the experimental program. Fig. 6 shows the geometry of the seawall used for numerical investigation.

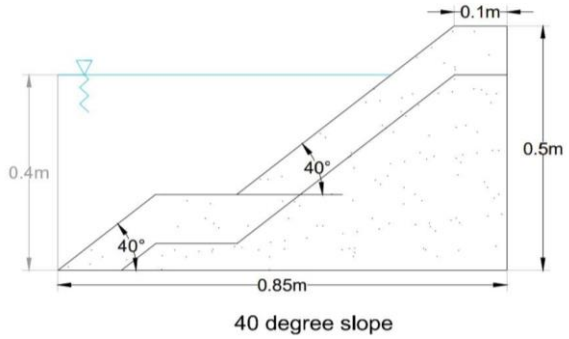

Fig. 6 Schematic sketch of slopes of seawall for Numerical investigation

Separate meshing is adopted for fluid and structure for the analysis. In the structure domain, a simple rectangular meshing is created with a face sizing of 20 mm and an element size of 40mm. Fluid-Solid Interface (FSI) is created on the surface of the seawall facing the waves. The boundary conditions are defined by assigning fixed supports to 8 side faces of the seawall, excluding the face experiencing the wave attack.

In the VOF domain, a tetrahedron mesh (Fig. 7) is created. Finer meshing helps to catch the wave pressure values on the seawall structure where the wave impacts. The mesh is kept fine towards the fluid-solid interface, and it gradually increases towards the inlet of the flume. The bottom boundary condition is fixed as default in the VOF method, and the structure is assigned fixed support in the FEM domain.

The mesh convergence study has been done considering the wave theory parameters. The mesh sizes are altered and checked for wave theory is applied before solving the Navier Stokes equation. The body sizing towards the coarsest mesh is 100 mm, and the minimum sizing is 18 mm and near the FSI. Due to tetrahedral graded meshing, the total number of elements could be restricted to 17872, with a total of 3654 nodes in the fluid domain. Care is taken to divide the structure into a minimum of 3 parts at the most coarse mesh location. With this element size, effective convergence is observed. With meshing coarser than 18mm minimum size, the residuals of the k-epsilon and VOF model showcased divergence after 500-time steps. The total number of elements in the structural domain, including the zone of fluid-solid-interface tried, are 251200, 33250, 10982, and 4950 against element sizes of 10mm, 20mm, and 30mm, 40mm. Total nodes generated are 1046059, 143456, 49022, and 2678 respectively, with each mesh size. The computational time associated with 20 mm size, which is adopted for further calculations, is 2 hours 25 minutes.

The Navier-Stokes equation, which is a basis of fluid in vector form, is given as-.

$$P\left(\frac{dy}{dx} + v.\nabla v\right) = -\nabla P + \mu\nabla^2 + f \quad \text{.....(5)}$$

Where, P = Fluid pressure = Pascal or N/m2
Fluid Velocity = m/s
μ=dynamic viscosity = Pa.S (μ is the SI unit for dynamic viscosity - Pascal-second (Pa-s). Calculated as force (N) per unit area (m2) divided by the rate of shear (s-1).)
F = Total Force (N)
The continuity equation in 2D Cartesian coordinates is given by:

$$\frac{\partial u}{\partial x} + \frac{\partial v}{\partial y} = 0 \text{..... (6)}$$

The boundary conditions of the flume, along with the fluid property, are assigned after meshing the domain. From the VOF Sub-Models, Open Channel Wave Boundary Conditions are selected.

The wave boundary condition can be set as Shallow Waves, Shallow/Intermediate Waves, and Short Gravity Waves. Wave can be simulated by using Wave Theories. Wave Theories are generally designated for simulating regular waves. To simulate random waves, the wave

spectrum is selected. In the present simulation, shallow/intermediate waves are simulated by using wave theories having 0.4 m water depth, 0.1m wave height, and 3.43 m wavelength.

The validity of wave theory is ascertained at this step, chiefly that the wave doesn't break before attacking the structure and impacts after travelling the length of the flume.

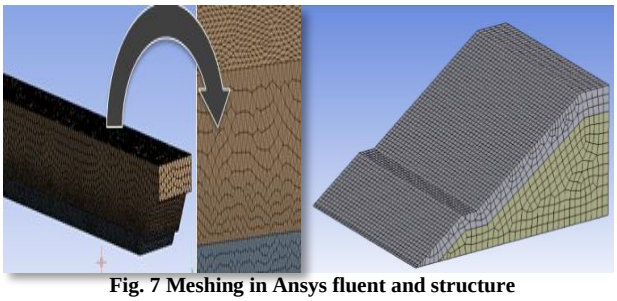

Fig. 7 Meshing in Ansys fluent and structure

The wave generation parameters are assigned to the water phase of the domain. In solver selection, the density-based solver is avoided as the fluid is not incompressible. Although solving the continuity, momentum, and energy equation simultaneously at the cost of time would offer a relatively accurate solution, the prime reason for utilising a pressure-based solver is pertaining to the wave theory assumptions that the fluid is incompressible. The pressure-based solver sequentially solves the set of continuity, momentum, and energy equations. First, it decouples the equations. Thereafter it solves the pressure-velocity coupling problem.

Continuity equation –

$$\frac{\partial \rho}{\partial t} + \nabla (\rho V) = 0 \ldots\ldots\ldots\ldots\ldots\ldots\ldots,.. (7)$$

Momentum equation –

$$P \frac{dV}{dt} = \rho g - \nabla p + \nabla \tau \ldots\ldots\ldots\ldots\ldots\ldots (8)$$

Energy-

$$\rho \frac{\partial e}{\partial t} + \rho (\nabla V) = \nabla (k \nabla T) + \varphi \ldots\ldots\ldots\ldots (9)$$

Where, P =pressure of fluid, ρ = density of fluid, g = acceleration due to gravity, V = Velocity of fluid, τ = Shear stress, T = change in temperature.

Thereafter, a transient time state is selected for the simulation since the steady-state disregards several cross requisites and higher-order requisites allocating time. These all terms get auto set to zero in steady-state so as to not affect the steady-state results. These terms are included in a transient simulation.

The volume of fluid (VOF) and Viscous K-epsilon (k-ε) model are used. The VOF model can model two or more two immiscible fluids by resolving a single set of momentum equations and following the volume fraction of each of the fluids throughout the domain.

The (k-ε) model is a two-equation model that gives an overall explanation of turbulence utilising two transport equations. The first transported variable is the turbulence kinetic energy (k). The second transported variable is the amount of dissipation of turbulence energy (ε).

Four waves are generated (Fig. 8) using the inbuilt open channel wave boundary conditions, using hybrid initialisation, which is based on Laplace's Equation to establish the pressure and velocity parameters.

Laplace equation

$$\frac{d\varphi}{dt} = -g\eta + \frac{1}{2}[\Delta\varphi]^2 \ldots\ldots\ldots\ldots\ldots\ldots (10)$$

Where φ = velocity potential

In hybrid initialisation, all other variables, such as temperature, turbulence, volume fractions, etc., will be patched built on domain averaged values or a specific interpolation technic. The Solution initialisation allows the solver to guess the solution and make a guess of the solution flow field and thus an integral part of numerical simulation to achieve faster convergence.

Thereafter the cell zone conditions are defined. It aids in the selection of water wave zone and inserting the numerical beach inputs in the base of the numerical flume.

The readings of the first 2 waves are discarded for jump start conditions, and the latter two are selected. The solution report is generated when the solution is converged. The results of the generated wave are coupled as an input for the FEM structure.

To foresee the effect of generated waves on the structure, the system of VOF is coupled with FEM. The force developed due to wave characteristics influenced by the slope of the structure needs to be fed into the structural analysis domain of the tool. This way, a one-way coupling of the system is performed.

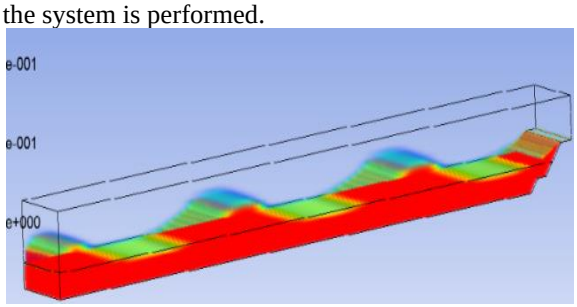

Fig. 8 Wave generated in the VOF domain of the numerical tool

The soil properties are assigned to the structural geometry, as shown in table 3. The density is calculated in the lab using the standard proctor test; corresponding characteristics of soil with similar density were taken from inbuilt data sets of the tool.

Table 3. Soil Properties applied to the seawall

Properties of Soil	
Density	1680 kg/m^3
Young's modulus	1.15 MPa
Poisons ratio	0.0279
Bulk modulus	1.5083 x 10^6 Pa
Shear Modulus	7.8186 x 10^5 Pa
Compressive strength	1.5 MPa

While transferring the pressure from VOF to the FEM domain through the FSI, the shift of meshing style ensured the effective transmission of force to the structure [48]. The structure failed to resolve forces when meshed in a tetrahedral style due to bad interconnection between the changing domains and material properties in the solver.
After the solver takes the input from the VOF solution and solves equation 8.

$$\delta = \frac{F \times L}{E \times A} \quad \ldots\ldots\ldots\ldots\ldots\ldots\ldots\ldots\ldots\ldots\ldots\ldots.. (11)$$

Where, δ = Total deformation, F= Force over the structure, L = Length, E = Modulus of Elasticity, A = Cross Section area of Seawall.

The force is obtained by dividing pressure by the area over which it impacts. It acts on the centre of the FSI plate. With the change in the slope of the seawall, the surface area of the frontal face of the seawall would also change, and therefore the value of total deformation would change in direct proportion to the surface area for the same set of wave parameters. However, the computation of the value of force requires accurate modelling of the wave generated and thereby the force exerted.

3. Results and Discussion

The calibrated numerical model is first compared with analytical, empirical equations. The equations, which are a result of experimental analysis on sloping structures, are incorporated. The following equations represent wave force, especially with no overtopping [5].

$$F = \rho\, g\, H \times (0.42 + 0.15\frac{\tan\theta}{\sqrt{H/L}}) \times A \;\ldots\ldots(12)\ [35]$$

$$F = (0.89 \times \{f + 1.2\}) \times \rho \times g \times d' \times \sin^2\theta \times A..(13)\ [49].$$

$$F = 2.8 \times \rho \times g \times h \times \sin^2\theta \times A\ldots\ldots(14)\ldots\ldots\ldots.[49].$$

Where,
ρ = Density of ocean water kg/m^3,
g = Acceleration due to gravity m/s^2,
H = Wave height with water depth,
$\frac{\tan\theta}{\sqrt{H/L}}$ = ξ = Surf similarity parameter,
A = Area of seawall where wave impacted,
d' = Water depth,
θ = Slope angle of seawall,
f = 1.8.

The analytical result of pressure for a 26-degree slope is calculated to be 6.17 millibars. Corresponding numerical and experimental results obtained are 7.159 millibars and 6.82 millibars, respectively, as shown in Fig. 9.

Therefore, the analytical and experimental results numerical results have less than a 10 per cent deviation in the values. This implies that the analytical, numerical, and experimental outcomes for the considered Irribaren number of 0.1528 (corresponding to a 26-degree slope) are in good agreement with each other. Therefore, using the calibrated model, the slope of the seawall is changed, and the total deformation of the seawall could be calculated analytically for the varying value of α, that is, 40^0, 45^0,50^0,55^0 and 60^0, using equation 5. The term A changed according to the varying slope to give variation in deformation values. The results were compared with those obtained numerically, as shown in table 4. It is observed that the values match well.
The results obtained from equations 12 to 14 for varying slopes are compared to those generated by the numerical tool and tabulated in table 5.

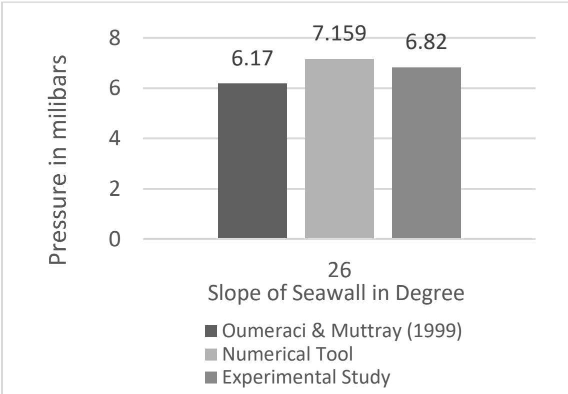

Fig. 9 Comparison between analytical, numerical, and experimental results for pressure calculated at surf similarity parameter 0.1528 (i.e. for slope angle 26^0)

Table 4. Analytical and numerical calculation of Total Deformation

Surf Similarity Parameter	Total Deformation (Analytical method)	Total Deformation of Seawall (mm) (Numerical Method)
4.92	1.46mm	1.45115mm
5.857	1.44 mm	1.4558mm
6.9795	1.52mm	1.4919mm
8.364	1.705mm	1.7113mm
10.144	1.71 mm	1.72875mm

The pressure calculated analytically is 2.5185 millibar. From the experimental investigation, the pressure result recorded using the pressure transducer is 6.82 millibars which is equivalent to 0.000682N/mm^2 or 682 pascals.

The results of total deformation calculated analytically and numerically are as shown in Fig. 10. The results are in good agreement with those obtained from the numerical tool. This is because the deformation is a function that is directly proportional to the force acting on the seawall and the length of the structure and inversely proportional to the cross-sectional area over which it acts, as well as the modulus of elasticity of the structure. Thus the wave conditions are simulated accurately, thereby generating an accurate force on the seawall and, therefore, the deformation.

After multiple trials on the selection of time step and step size on the VOF model, adopting a smaller time step results in the convergence of the solution. However, a very small time step can put a burden on the processor as well, as it will be more taxing in terms of time to reach converge. After multiple iterations, the optimal time for the current case is found to be 0.09 seconds.

Table 5. Analytical Results of Wave Force (N)

ξ	Muttray, M., &Oumeraci, H. (1999)	(Hom-ma, M., & Horikawa, K. (1964))	(Hom-ma, M., &Horikawa, K. (1964))*	Force (N)
4.92	2353.53	2831.57	3536.95	1738.2
5.86	2316.05	3109.95	3884.66	1924
6.98	2335.26	3363.02	4207.02	2000
8.36	2411.91	3601.09	4498.15	2046.3
10.144	2560.175	3808.95	4757.8	2109

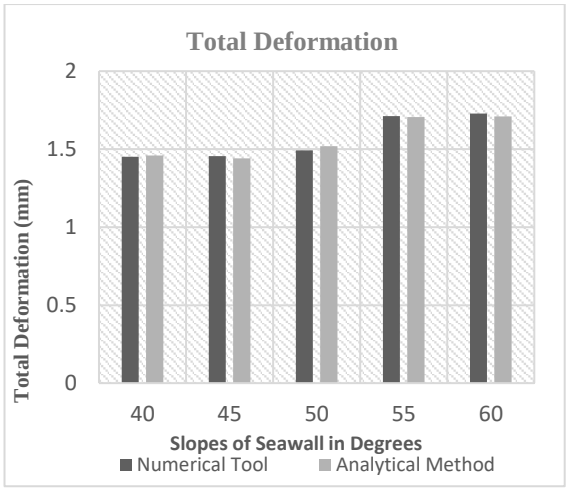

Fig. 10 Numerical and analytical results of total deformation of seawall

Any time step larger than this time resulted in an unstable model, and peak divergence, especially in the KE model, is observed due to which the run terminated frequently. Also, the number of time steps, if kept less, results in the divergence in the model as the next iteration is begun before reaching an optimised solution of the previous step, thereby leading to the failure of the model. Thus, after multiple trials, the optimal iterations were set to 45 for the current case. As the solver reached an optimal solution within 20-25 steps, it prompted for a converged solution and skipped the remaining iterations, and jumped on to the next step.

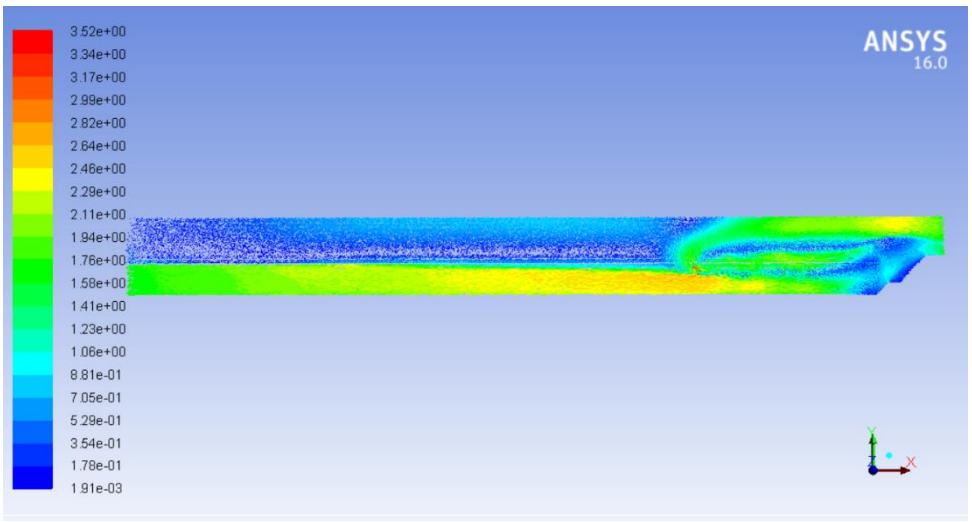

Fig. 11 The repulsed waves in the wave flume

Fig. 11 shows the mixing of the velocity vectors of the wave after it is repulsed from the structure. A closer look at the velocities can be seen in Fig. 12. This is a key feature when no waves are allowed for transmission. All the wave vectors will rebound and mix with approaching waves to create turbulence downstream of the seawall. This is also the reason for accounting for a scour protection device. The force imported into the seawall (Fig. 13) has a maximum value at the bottom of the seawall due to the turbulence because of rebounded waves. The maximum value of force on the structure is used for comparison with the empirical equations.

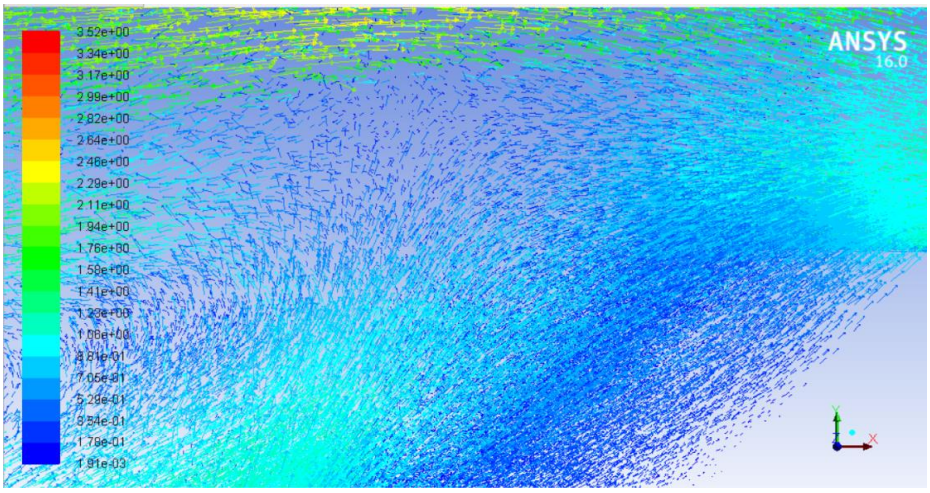

Fig. 12 The repulse of water vectors in the model

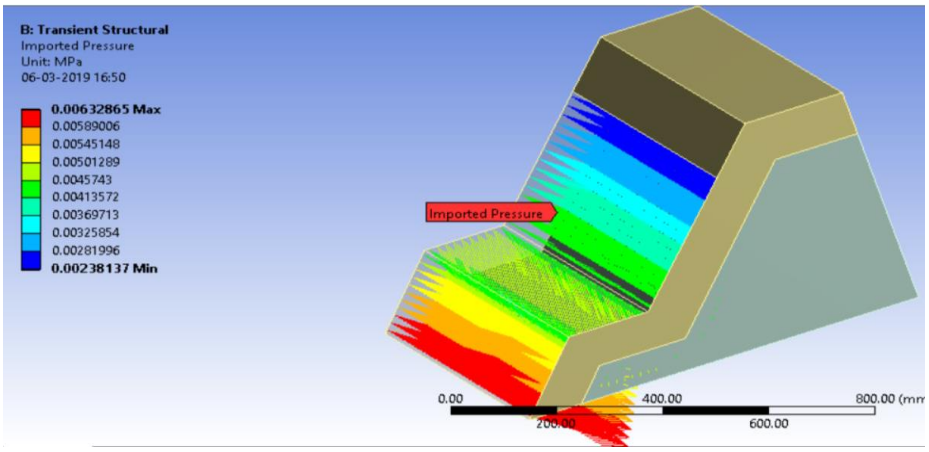

Fig. 13 The imported pressure on seawall due to coupling

The resolved force is obtained from the numerical simulation and is used for the coupling. The solver failed with the adoption of the tetrahedral meshing of the seawall. This is because of the convoluted meshing boundaries. The deformation profile obtained in Fig. 14 is a result of simplified square meshing for coupled systems. The highest value of pressure is experienced at the toe due to the repulse of the wave from the seawall body. Nevertheless, the maximum deformation resulting from the maximum pressure on the seawall would be at the centre of the structure.

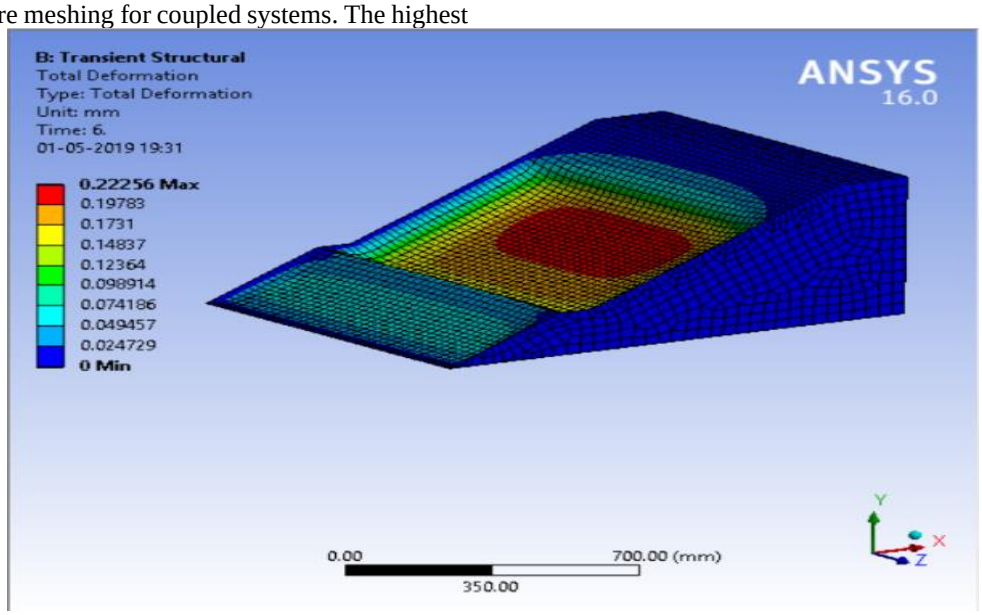

Fig. 14 Total deformation profile of the seawall

Fig. 15 shows the variation of slope along with the abscissa and corresponding force values on the ordinate obtained numerically as well as analytically. The trend is in good agreement with the numerical results, and the results obtained by equation 9 are in better agreement than equations 10 and 11. The root mean square error value for results compared with [35] equation 9 is 0.197. As compared to (Homma & Horikawa, 1964), the RMSE value using equation 9 is 1.954, and a higher RMSE value is obtained from equation 11, which is 4.99. This is because of the introduction of the factor "f" in equation 10, which is a modified equation of wave force on the sloping surface. The correlation coefficient of the force obtained by [35] with the numerical model is 0.632. Homma & Horikawa, 1964) force values are strongly correlated with a correlation coefficient of 0.968 with the numerical force values.

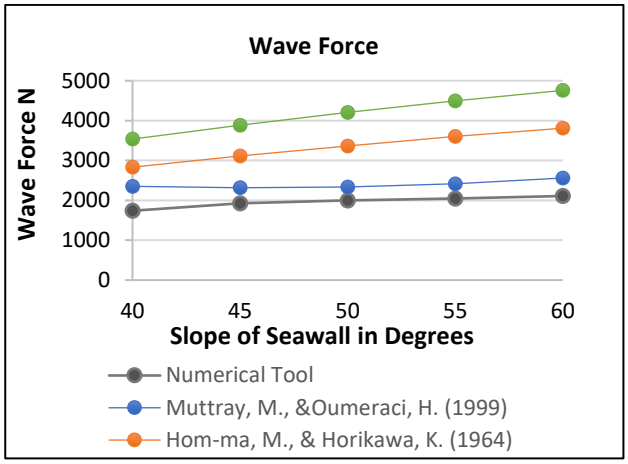

Fig. 15 Comparison between analytical and numerical results of wave force

4. Conclusion

Numerical methods for the study of wave-structure interaction are utilised widely over the globe. The selection of a particular computational method from the expanse of technics available is usually finalised based on the parameters desired to be studied using the tool. For studying the response of the structure to the impounding wave, extensive research is available, which is performed using experimental setups. Along with these experimental investigations, many of the studies are performed using numerical investigations, and the results are plotted as a function of Irribaren number ξ, which in turn is a function of wave height, wavelength, and slope of the seawall. In the Irribaren number itself, the variation performed is that of the wave parameters and not the slope. This is because; it is experimentally exhausting to change the physical properties and dimensions repeatedly in the wave flume. Therefore numerical investigation techniques would be an ideal solution for saving immense labour and experimentation costs involved, especially when the research needs to be focused on the structural parameters.

Various numerical investigations are performed on offshore structures or shoreline structures, allowing wave transmission. However, no work is carried out using coupled VOF-FEM on non-wave transmitting structures in shallow water regions, wherein the response of the structure to the impacted wave can be noted. Further, the effect of energy dissipation concerning the changing slope is not carried out numerically.

In the present study, a regular wave is imparted on the structure to evaluate the force and corresponding deformation of the structure. The flume length of 10 m is sufficient when studies are focused on structure performance, mainly wave impact or overtopping studies. A longer-length flume would be deemed necessary when reflection [4] studies or sediment transport needs to be evaluated. An experiment is performed to use reference values for the numerical simulation model of the smooth impermeable seawall with no overtopping and complete reflection using standard procedure [50]. Predominantly the effect of the slope of the seawall α with total deformation is checked. Total deformation is calculated numerically for changing values of α (α= 40º, 45º,50º,55º, and 60º) of the seawall. The wave characteristics are kept consistent. The total deformation and wave forces on the seawall increase with an increase in the slope of the seawall.

It is observed that existing empirical equations predict the wave force quite accurately. However, there is a significant difference in the results obtained by numerical tools and equations 13 and 14. This is because equation 12 has the entire Irribaren number term, and thereby the force is calculated considering the characteristics of the wave as well as the slope of the seawall. Whereas in equations 13 and 14, the term Θ which is the slope of the seawall, exists, but the wave characteristics are normalised with constants from their empirical derivations. These equations overestimate the wave force on the seawall. Therefore, it implies that the Irribaren number is the most influential parameter when it comes to wave structure interaction on a sloping coastal structure.

For successful implementation of VOF-FEM coupling for fully wave reflecting structures like a seawall, the meshing region of the VOF domain could be kept as graded meshing, keeping it finer at the fluid-solid interaction interface and coarser at the origin. At least 3 divisions of the influent region shall be ascertained for a clear convergence of the solution. For studies with regular wave impact on the structure, the transient time state is ideal to be adopted. The structure needs to have simple meshing for the effective transfer of wave force onto the structure. The dynamic force acts perpendicular to the structure. The time step of 0.09 with 45 iterations per time step is deemed sufficient for this study to provide convergence and successful readings. Due to the repulse of waves, turbulence is created on the downstream side of the seawall. This can be managed by the provision of numerical beaches in the near-seawall region. Since the study of structure response can be achieved by regular wave impact, a single significant wave can be generated in the numerical domain. It is suggested that the flume length can be divided by the calculated length of the wave to be generated, thereby reducing computation time for developing force on the structure.

The future scope of the work perchance utilises the technic for two-way coupling of the system for a further deeper understanding of the wave structure interaction. The study of structural response for service life performance assessment can be extended to using random waves as input or regular waves of the amplitude values that of significant or extreme waves. This can help in defining the ultimate stability and response of the structure to extreme waves in field conditions. This can especially be utilised for permeable structures for which very few studies are done hitherto.

Acknowledgment

The authors are grateful to Symbiosis International (Deemed University) for providing grants under the Student Research Project (SIU-SRP-1139) for supporting the experimentation part of this research.

Conflict of Interest

On behalf of all authors, the corresponding author states that there is no conflict of interest.

References

[1] Coastal Engineering Research Center, Shore Protection Manual US Army Corps of Engineers, Coast. Eng., I (1984) 1–337. [Online]. Available: http://ft-sipil.unila.ac.id/dbooks/S P M 1984 volume 1-1.pdf.
[2] S. P. Manual, Shore Protection Manual - Volume 1, Dep. Army, 1(2) (1984) 337, doi: 10.5962/bhl.title.47830.
[3] S. Neelamani, K. Al-Salem, and A. Taqi, Experimental Investigation on wave Reflection Characteristics of Slotted Vertical barriers with an impermeable back wall in random wave fields, J. Waterw. Port, Coast. Ocean Eng., 143(4) (2017) 1–10. doi: 10.1061/(ASCE)WW.1943-5460.0000395.
[4] A. Negm and K. Nassar, Determination of Wave Reflection Formulae for Vertical and Sloped Seawalls Via Experimental Modelling, Procedia Eng., 154 (2016) 919–927, doi: 10.1016/j.proeng.2016.07.502.
[5] K. Nassar, W. E. Mahmod, A. Tawfik, O. Rageh, A. Negm, and H. Fath, Developing Empirical Formulas for Assessing the Hydrodynamic Behaviour of Serrated and Slotted Seawalls, Ocean Eng., 159 (2018) 388–409, doi: 10.1016/j.oceaneng.2018.04.048.
[6] V. Mallayachari and V. Sundar, Reflection Characteristics of Permeable Seawalls, Coast. Eng., 23(1–2) (1994) 135–150, doi: 10.1016/0378-3839(94)90019-1.
[7] V. Gruwez et al., An Inter-model Comparison for Wave Interactions with Sea Dikes on Shallow Foreshores, J. Mar. Sci. Eng., 8(12) (2000) 1–37. doi: 10.3390/jmse8120985.
[8] F. M. Judge, A. C. Hunt-Raby, J. Orszaghova, P. H. Taylor, and A. G. L. Borthwick, Multi-Directional Focused wave Group Interactions with a Plane Beach, Coast. Eng., 152(2019) 103531, doi: 10.1016/j.coastaleng.2019.103531.
[9] M. Zijlema, G. Stelling, and P. Smit, SWASH: An Operational Public Domain code for Simulating Wave Fields and Rapidly varied flows in Coastal waters, Coast. Eng., 58(10)(2011). 992–1012, doi: 10.1016/j.coastaleng.2011.05.015.
[10] D. M. Skene, L. G. Bennetts, M. H. Meylan, and A. Toffoli, Modelling Water Wave Overwash of a thin Floating Plate, J. Fluid Mech. 777(2015) 1–13. doi: 10.1017/jfm.2015.378.
[11] T. Suzuki et al., Efficient and Robust Wave Overtopping Estimation for Impermeable Coastal Structures in Shallow Foreshores using SWASH, Coast. Eng., 122 (2017)108–123. doi: 10.1016/j.coastaleng.2017.01.009.
[12] D. F. A. Vanneste, C. Altomare, T. Suzuki, P. Troch, and T. Verwaest, Comparison of Numerical Models for Wave Overtopping and Impact on a Sea Wall, Coast. Eng. Proc., 1(34)(2014) 5. doi: 10.9753/icce.v34.structures.5.
[13] B. L. Dang, H. Nguyen-Xuan, and M. Abdel Wahab, Numerical Study on Wave Forces and Overtopping Over Various Seawall Structures using Advanced SPH-based method, Eng. Struct., 226 (2019) 111349, (2021), doi: 10.1016/j.engstruct.2020.111349.
[14] S. J. Lind, B. D. Rogers, and P. K. Stansby, Review of Smoothed Particle Hydrodynamics: Towards Converged Lagrangian flow Modelling: Smoothed Particle Hydrodynamics review, Proc. R. Soc. A Math. Phys. Eng. Sci., 476(2020) 2241, doi: 10.1098/rspa.2019.0801.
[15] Z. Liu and Y. Wang, Numerical Investigations and Optimisations of Typical Submerged box-type Floating Breakwaters using SPH, Ocean Eng., 209 (2020) 107475. doi: 10.1016/j.oceaneng.2020.107475.
[16] X. Y. Ni and W. Bin Feng, Numerical Simulation of Wave Overtopping Based on DualSPHysics, Appl. Mech. Mater., 405–408 (2013) 1463–1471. doi: 10.4028/www.scientific.net/AMM.405-408.1463.
[17] W. Finnegan and J. Goggins, Numerical simulation of linear water waves and wavestructure interaction, Ocean Eng., 43(2012) 23–31 doi: 10.1016/j.oceaneng.2012.01.002.
[18] J. Jiao and S. Huang, CFD Simulation of Ship Seakeeping Performance and Slamming loads in Bi-directional Cross wave," J. Mar. Sci. Eng., 8(5)(2020) 1–24, 2020. doi: 10.3390/JMSE8050312.
[19] M. Zabihi, S. Mazaheri, and A. R. Mazyak, Wave Generation in a Numerical Wave Tank, 17th Mar. Ind. Conf. 22-25 December 2015 – Kish Isl.,. 2(11), 2015.
[20] Y. M. Choi, Y. J. Kim, B. Bouscasse, S. Seng, L. Gentaz, and P. Ferrant, Performance of Different Techniques of Generation and Absorption of Free-Surface Waves in Computational Fluid Dynamics, Ocean Eng., 214 (2019) 107575. (2020) doi: 10.1016/j.oceaneng.2020.107575.
[21] J. Inverno, M. G. Neves, E. Didier, and J. L. Lara, Numerical Simulation of Wave Interacting with a Submerged Cylinder using a 2D RANS model, J. Hydro-Environment Res., 12(2016) 1–15. doi: 10.1016/j.jher.2016.02.002.
[22] T. W. Hsu, C. M. Hsieh, and R. R. Hwang, Using RANS to Simulate Vortex Generation and Dissipation Around Impermeable Submerged Double Breakwaters, Coast. Eng.,51(7)(2004) 557–579. doi: 10.1016/j.coastaleng.2004.06.003.
[23] J. H. Chow, E. Y. K. Ng, and N. Srikanth, Numerical Study of the Dynamic Response of a Wind Turbine on a Tension leg Platform with a Coupled Partitioned Six Degree-of-Freedom Rigid body Motion Solver, Ocean Eng., 172(2018) 575–582, (2019) doi: 10.1016/j.oceaneng.2018.12.040.
[24] J. L. Lara, P. Higuera, R. Guanche, and I. J. Losada, Wave Interaction With Piled Structures: Application With IH-FOAM, Vol. 7 CFD VIV, no. August, p. V007T08A078, (2013) doi: 10.1115/OMAE2013-11479.

[25] Z. Z. Hu, D. Greaves, and A. Raby, Numerical wave tank Study of Extreme Waves and Wave-structure Interaction using OpenFoam®," Ocean Eng., 126 (2015) 329–342, (2016). doi: 10.1016/j.oceaneng.2016.09.017.
[26] L. F. Chen, J. Zang, A. J. Hillis, G. C. J. Morgan, and A. R. Plummer, Numerical investigation of wave – Structure Interaction using OpenFOAM, Ocean Eng., 88(2014) 1950 91–109. doi: 10.1016/j.oceaneng.2014.06.003.
[27] G. Zhang, X. Chen, and D. Wan, MPS-FEM Coupled Method for Study of Wave-Structure Interaction, J. Mar. Sci. Appl., 18(4)(2019) 387–399, doi: 10.1007/s11804-019-00105-6.
[28] I. C. Chien, S. P. Wu, H. C. Ke, S. L. Lo, and H. H. Tung, Comparing Ozonation and Biofiltration Treatment of Source Water with High Cyanobacteria-Derived Organic Matter: The Case of a Water Treatment Plant followed by a Small-Scale Water Distribution System, Int. J. Environ. Res. Public Health, 15(12), (2018) doi: 10.3390/ijerph15122633.
[29] J. Liu and G. Lin, Scaled Boundary FEM solution of Short-Crested Wave Interaction with a Concentric Structure with Double-layer arc-Shaped Perforated Cylinders, Comput. Fluids, 79(2013)82–104. doi: 10.1016/j.compfluid.2013.03.013.
[30] C. Engineering and U. Planning, Numerical Simulation of Regular Waves Run-Up Over Slopping Beach By Open Foam, An Int. J., 1, 1(2014)
[31] T. Bunnik, Omae2016-54808, (2017) 1–12.
[32] C. Zhang, N. Lin, Y. Tang, and C. Zhao, A Sharp Interface Immersed Boundary/VOF model Coupled with Wave Generating and Absorbing options for Wave-Structure Interaction, Comput. Fluids, 89(2014)214–231. doi: 10.1016/j.compfluid.2013.11.004.
[33] H. Moayedi, B. B. K. Huat, T. A. M. Ali, Z. Bakhshipor, and M. Ebadi, Comparison of Geotube and Stone Cemented wall Stability as Coastal Protection System [case study and 2D limit equilibrium and FEM modeling analysis], Aust. J. Basic Appl. Sci., 5(7)(2011) 1–6.
[34] X. Zhao, X. Wang, and Q. Zuo, Numerical Simulation of Wave Interaction with Coastal Structures using a CIP-based Method, Procedia Eng. 8th Int. Conf. Asian Pacific Coasts, 116(1)(2015). 155–162. doi: 10.1016/j.proeng.2015.08.277.
[35] M. Muttray and H. Oumeraci, Prediction of wave Pressures on Smooth Impermeable Seawalls, 26(1999) 739–765.
[36] Q. Du and D. Y. C. Leung, 2D Numerical Simulation of Ocean Waves, Mar. Ocean Technol.(2011)2183–2189. doi: 10.3384/ecp110572183.
[37] G. Mayra, No Title No Title, J. Chem. Inf. Model., 53(9)(2013) 1689–1699.
[38] Marine Sanctuaries Conservation Series, The Impacts of Coastal Protection Structures in California's Monterey Bay National Marine Sanctuary,
(2005).
[39] M. Zabihi, S. Mazaheri, and A. R. Mazyak, Wave Generation in a Numerical Wave Tank, 17th Mar. Ind. Conf. 22-25 December 2015 – Kish Isl., 2(11) (2015) [Online].Available:https://www.researchgate.net/publication/288280408.
[40] T. J. Wipf et al., Design Recommendations for the use of FRP for Reinforcement and Strengthening of Concrete Structures, Constr. Build. Mater., 5(1)(2016) 16–28 doi: 10.1002/pse.139.
[41] K. O. Connell and A. Cashman, Development of a numerical wave tank with reduced discretisation error, Int. Conf. Electr. Electron. Optim. Tech. ICEEOT (2016) 3008–3012, doi: 10.1109/ICEEOT.2016.7755252.
[42] 367 Hydro Patana Full Length Paper .(2018).
[43] T. V. Karambas and A. G. Samaras, An Integrated Numerical Model for the Design of Coastal Protection Structures, J. Mar. Sci. Eng., 5(4)(2017). doi: 10.3390/jmse5040050.
[44] H. E. Williams, R. Briganti, A. Romano, and N. Dodd, Experimental Analysis of wave Overtopping: A new Small Scale Laboratory Dataset for the Assessment of Uncertainty for Smooth Sloped and Vertical Coastal Structures, J. Mar. Sci. Eng., 7(7)(2019)1–18. doi: 10.3390/jmse7070217.
[45] F. Azarsina, A. Pirzadeh, and G. Darvish, Small Scale Physical Measurement of Wave Overtopping For Different Shore Protection Structures, Int. J. Marit. Technol., no. Summer and Autumn 12(2019) 49–56. doi: 10.29252/ijmt.12.49.
[46] T. Suzuki, M. Tanaka, and A. Okayasu, Laboratory Experiments on wave Overtopping over Smooth and Stepped Gentle Slope Seawalls, Asian Pacific Coasts, (2003) - Proc. 2nd Int. Conf., no. (2004) doi: 10.1142/9789812703040_0078.
[47] SPM, Shore Protection Manual Waterways Experiment Station , Corps of Engineers, Dep. Army, Waterw. Exp. Station. 1 (II)(1984).
[48] H. Oumeraci and A. Kortenhaus, Core made of geotextile sand containers for rubble mound breakwaters and seawalls: Effect on armour stability and hydraulic performance, Ocean Eng., 38(1)(2011) 159–170. doi: 10.1016/j.oceaneng.2010.10.014.
[49] M. Hom-ma and K. Horikawa, Wave Forces Against Sea Wall, pp. (1964)490–503.
[50] W. Allsop, Wave reflections from coastal structures., Odu Bull.,. 16(6) (1989). doi: 10.1142/9789812709554_0364.